JOURNAL OF SOLID STATE CHEMISTRY 19, 67–73 (1976)

Determination of the Diffusion Coefficients from Sintering Data of Ultrafine Oxide Particles

M. ASTIER AND P. VERGNON

Université Claude Bernard (Lyon I), Laboratoire Associé au CNRS n° 231, Catalyse Appliquée et Cinétique Hétérognèe, 43, boulevard du 11 novembre 1918, 69621 Villeurbanne, France

Received November 14, 1975; in revised form, May 17, 1976

Many kinetic equations derived from a simple geometrical model can account for the shrinkage rate of pellets of particles. Nevertheless, even when a kinetic equation is followed the calculation of the apparent diffusion coefficient may not be meaningful if the system under study and the theoretical model does not fit closely. This is shown by the experimental results on sintering of fine particles of anatase and alumina. When the system closely fits the model, the predicted sintering equation is observed and the calculated diffusion coefficients are close to the cation diffusion coefficients. But when the system (polyhedral particles) does not fit the model, an apparent agreement is found between the experimental results and the theoretical law corresponding to an unrelated model so that the calculated diffusion coefficient is meaningless.

The word "sintering" covers many complex phenomena and their scientific approach requires the use of simplified models. Such models allow an establishment of relationships between some geometrical parameters of the system and the time of sintering when a suitable mechanism for material transport is assumed. But the equations which apply to the sintering of spheres, for example, cannot be applied in the case of lamellar or porous bodies. Similarly, in the case of very small particles (less than 1000 Å) some of the hypotheses which are convenient for large particles cannot be applied any more and others models must be proposed (*1*).

The determination of the diffusion coefficients (when the mechanism for the material transport is diffusion) from kinetic equations of sintering (shrinkage of pellets versus time, for instance) is possible only when the hypotheses used in these equations are stated precisely and are justified. In this work the values of the apparent diffusion coefficients, calculated from the isotherms of shrinkage of titanium dioxide and alumina compacts, are discussed and compared with the values of diffusion coefficients of the anion and the cation in the corresponding oxide.

Kinetic Equations for the Sintering of Spherical Particles

Many sintering models have been proposed to derive the shrinkage rate of compacts of spherical particles. In most cases the starting point is the calculation of the stress normal to the junction area of the particles. In the case of two grains bound by a flat junction area and having a symmetry axis perpendicular to this area, the stress normal to this junction area is (by supposing mass transport by diffusion):

$$\sigma(r) = \frac{Kr^2}{4} + C, \qquad (1)$$

where r is the distance from the symmetry axis and K and C are two constants. A particular value of $\sigma(r)$ is $\sigma(x)$ for $r = x$ (x is the radius of the junction area):

$$\sigma(x) = -\left(\frac{1}{R_1} + \frac{1}{R_2}\right) \tag{2}$$

and

$$\sigma(r) = \frac{K}{4}(r^2 - x^2) - \gamma\left(\frac{1}{R_1} + \frac{1}{R_2}\right). \tag{3}$$

R_1 and R_2 are the principal radii of curvature of the grain surface at the intersection of two particles and γ is the surface tension. In order to calculate K, a second boundary condition must be known. This boundary condition may be, for example, a particular value of the stress $\sigma(r_0)$ at a given distance r_0 from the center of the particles. The stress is then given by

$$\sigma(r) = \sigma(r_0)\frac{r^2 - x^2}{r_0^2 - x^2} + \gamma\left(\frac{1}{R_1} + \frac{1}{R_2}\right)\frac{r^2 - r_0^2}{r_0^2 - x^2} \tag{4}$$

and the flux of atoms (atoms crossing a unit of the surface per unit of time) is related to the stress gradient (*2*) for $r = x$,

$$j = -\frac{D}{kT}\left(\frac{d\sigma(r)}{dr}\right)_{r=x}, \tag{5}$$

using Eq. (*4*):

$$j = -\frac{D}{kT}\left(\gamma\left(\frac{1}{R_1} + \frac{1}{R_2}\right) + \sigma(r_0)\right)\frac{2x}{r_0^2 - x^2}. \tag{6}$$

Microscopic observations of spherical particles in contact shows the formation of a neck between two particles during the initial stage of the sintering (*3–5*). Kuczynski (*3*), by writing that the vacancy concentration gradient is inversely proportional to the curvature radius ρ of the neck, assumed that the neck is the source of vacancies which disappear at a distance of the same order of magnitude as the radius of curvature. With these conditions, using Eq. (6) ($R_1 = x$, $R_2 = -\rho$, $r_0 = x - \rho$, $\sigma_{(r_0)} = 0$), the flux is given by (Fig. 1)

$$j = \frac{D}{kT}\gamma\left(\frac{1}{x} - \frac{1}{\rho}\right)\frac{2x}{\rho(\rho - 2x)}, \tag{7}$$

and as ρ is much smaller than x

$$j = \frac{-D\gamma}{kT\rho^2}. \tag{8}$$

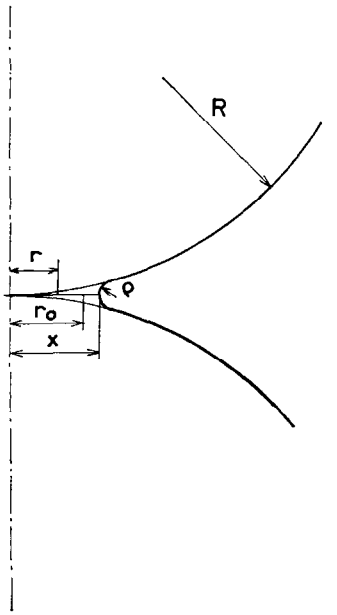

FIG. 1. Model of tangent spheres with the formation of a neck.

The neck radius is related to time by

$$\frac{x^5}{R^2} = \frac{40\gamma D\Omega}{kT}t, \tag{9}$$

where Ω is the vacancy volume and $\rho \sim x^2/(2R)$ (Fig. 1). Kingery and Berg (*6*) obtained the same equation but they applied it to the shrinkage of two particles in contact. The equation for the shrinkage ratio is then

$$\frac{\Delta L}{L_0} = \frac{20}{2^{\frac{1}{2}}}\left(\frac{\gamma\Omega D_v}{R^3 kT}t\right)^{2/5}, \tag{10}$$

The hypotheses which permitted the establishment of Eqs. (9) and (10) make it impossible to use these equations to described the shrinkage. Moreover, it has been shown that the assumptions leading up to Eqs. (9) and (10) are entirely inappropriate (*7, 8*). Nevertheless, the time dependence for neck growth or shrinkage in these equations has been observed (*5, 9, 10*).

The distance between the centers of two particles can only decrease when the material transport takes place from the center of the junction zone to the neck surface. In this case, a stress is exerted by a particle upon another at

the center of the junction area. The boundary condition can be obtained from the condition of equilibrium of the grain boundary (*11*, *12*)

$$2\pi \int_0^x \sigma(r) r\, dr = 2\pi x\gamma \cos\alpha, \qquad (11)$$

where $\alpha = (\pi - \beta)/2$ and β is the grain boundary groove angle.

Two cases can be considered according to the size of the particles:

(a) R is large and a neck is formed between the particles (Fig. 2, the most general case in sintering experiments).

If $\alpha \sim 0$, Eq. (11) gives

$$\sigma(0) = \gamma\left(\frac{1}{x} - \frac{1}{\rho}\right) + \frac{4\gamma}{x}. \qquad (12)$$

x and ρ are the main radii of curvature of the neck.

An equation which takes into account both volume and grain boundary diffusion has been given by Johnson (*11*):

$$y^{2.06}\dot{y} = \frac{2.63\gamma\Omega D_v}{kTR^3} y^{1.03} + \frac{0.70\gamma\Omega D_B}{kTR^4} \qquad (13)$$

if $y = \Delta L/L_0$ for less than 4% shrinkage. D_v and D_B can be determined from the slope and the intercept of the plot $y^{2.06}\dot{y}$ versus $y^{1.03}$.

(b) R is small and no neck is formed between the particles.

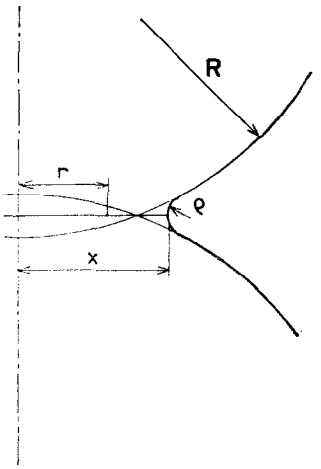

FIG. 2. Model of secant spheres with formation of a neck.

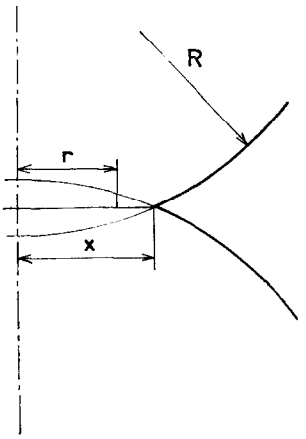

FIG. 3. Model of secant spheres.

In the case of very small spherical particles ($R < 1000$ Å) a study by electron microscopy (*13*) shows that no neck with a negative radius of curvature is formed between the particles. The geometry of the system is described by two secant spheres as shown in Fig. 3, and $R_1 = R_2 = R$ (main radii of curvature near the junction area of the two particles). Moreover the boundary condition (Eq. (11)) is now:

$$2\pi \int_0^x \sigma(r) r\, dr = 2\pi x\gamma \sin\theta,$$

where $\sin\theta = \cos\alpha$ and as $\sin\theta = x/R$

$$2\pi \int_0^x \sigma(r) r\, dr = 2\pi x^2/R.$$

With this condition, the stress at the center of the neck is

$$\sigma(0) = 6\gamma/R$$

and

$$j = 16D\gamma/(kTRx),$$

assuming radial diffusion in a cylinder.

The neck radius is related to time by

$$\frac{x^2}{2} = \frac{16\gamma D\Omega}{RkT} t. \qquad (14)$$

Such a relationship between neck size and time has been observed (*14*) in sintering study of submicron particles of alumina and zir-

conia by electron microscopy. The shrinkage ratio is then:

$$\frac{\Delta L}{L_0} = \frac{16\gamma D\Omega}{R^3 kT}. \qquad (15)$$

(c) R is still smaller ($R \sim 100$ Å).

In this case a study of the porosity of the compacts during sintering shows that the compact must be described as a porous polycrystalline body. If $\bar{l}$ is the average grain size and $\bar{r}$ is the average pore size, the order of magnitude of the shrinkage rate will be (assuming a Nabarro–Herring (*15*, *16*) microcreep mechanism):

$$\dot{y} \sim \frac{8\gamma D\Omega}{\bar{l}^2 kT\bar{r}}. \qquad (16)$$

The microscopic examination and the study of the porosity of compacts made with ultrafine particles of antimonium doped titanium dioxide show that $\bar{l}$ and $\bar{r}$ remain constant as long as a linear relationship between shrinkage and time is observed (*13*).

Equations (15) and (16) imply that all the hypotheses made in their derivation are satisfied and that surface diffusion can be neglected.

A formal experimental verification does not allow use of the kinetic equations, in particular for the determination of diffusion coefficients. In an actual compact, shapes and sizes of particles are various and some interparticular contacts (for example, plane over plane) do not cause shrinkage. In this case the total shrinkage is smaller than might be expected. Moreover, other phenomena can also occur, like particle rearrangement, which result in a more important shrinkage. It is therefore possible that the agreement between the theoretical and experimental laws is fortuitous.

Experimental

In order to test the applicability of the kinetic equations, the solids used for the sintering must be as well defined as possible. Samples of oxide powders of controlled shapes and sizes were prepared in an oxygen–hydrogen flame reactor (*17*) by decomposition of the corresponding metal chloride vapor. Doped samples are obtained from a mixture of chlorides. Characteristics of samples used are given in Table I.

Particles of anatase TiO_2A are spherical and nonporous and all have approximately the same size, whereas particles of anatase TiO_2B of similar surface area are very different in shape and size. Some of these particles are spherical but most of them present well-defined facets and their sizes are scattered between a few hundred and a few thousand Angströms.

The remaining anatase samples contain 0.1, 1.0, and 1.5 antimony atoms per 100 titanium atoms and the sample of alumina is made out of polyhedral particles (edges and facets). All these particles have a radius of about 100 Å.

The isothermal sintering of these samples is followed by a photographic measurement of the length of a compressed pellet (4 t/cm^2) heated in a few seconds up to the required temperature (*18*).

TABLE I

	TiO_2 A	TiO_2 B	TiO_2 Sb (0.1)	TiO_2 Sb (1)	TiO_2 Sb (1.5)	Al_2O_3
Specific area ($m^2 \cdot g^{-1}$)	10.6	13	86	85	82	132
Mean diameter,[a] d(Å)	1470	1200	180	180	190	170
Textural aspect	Spheres uniformly sized	Heterogeneous shapes and sizes		Polyhedrous uniformly sized		

[a] The mean diameter d is calculated from the equation $d = 6/Sp$, where S is the surface area and p is the density of oxide.

Kinetic results were published elsewhere (*18*). The initial stage of sintering, which corresponds to the formation of junctions between particles, takes place during the first 10 or 15 sec of the process, before the thermodynamic equilibrium is attained. Its study was presented separately (*19*).

Moreover, the study of the surface area change versus shrinkage (*13*, *19*) shows that surface diffusion is not a predominant mechanism in the case of the samples studied.

(a) TiO A: Spherical Particles

The isothermal shrinkage curves of pellets made with spherical particles present a linear part (*18*), which corresponds to the equation derived from the model of secant spheres without the formation of a neck. Moreover, the microscopic examination of particles during sintering shows that this model fits closely (*13*). It is thus possible to calculate the diffusion coefficient from Eq. (15). Between 750 and 825°C an apparent diffusion coefficient is given by (Fig. 4)

$$D = 108.6 \exp\left(\frac{-77140}{RT}\right) \text{cm}^2\,\text{sec}^{-1}.$$

(b) Alumina and Doped Anatase Samples

In the case of alumina and of doped anatase samples the isothermal shrinkage curves also exhibit a linear part (*18*). But the suitable model here is that of a polycrystalline body with pores. As the average radius of the pores is constant and close to the radius of particles (*13*), Eq. (16) must be used in order to calculate the order of magnitude of the diffusion coefficient. For alumina the apparent diffusion coefficient is expressed by (Fig. 5)

$$D = 1.4 \times 10^8 \exp\left(\frac{-158270}{RT}\right) \text{cm}^2\,\text{sec}^{-1}.$$

in the temperature range 1100 to 1300°C. In the case of the samples of titanium dioxide containing 0.1, 1.0, and 1.5% of antimonium, the apparent diffusion coefficients are, respectively (Fig. 4),

$$D = 27.5 \exp\left(\frac{-72220}{RT}\right) \text{cm}^2\,\text{sec}^{-1}$$

$$D = 83.3 \exp\left(\frac{-77560}{RT}\right) \text{cm}^2\,\text{sec}^{-1}$$

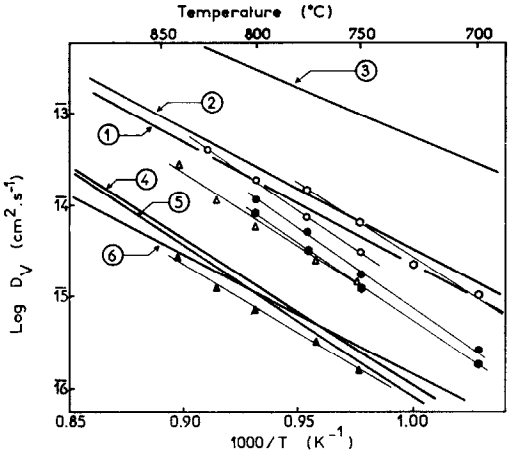

FIG. 4. Comparison of the diffusion coefficients calculated from the sintering data for TiO_2 with the diffusion data in the literature. Curve 1: ^{44}Ti in TiO_2 (*24*). Curves 2 and 3: D_{xx} and D_{zz} of ^{44}Ti in TiO_2 (*25*). Curves 4, 5, and 6: ^{18}O in TiO_2 (*23*). ○, sintering TiO_2 A from Eq. (*15*); △ and ▲, sintering TiO_2B from Eqs. (*13*) and (*10*), respectively; ○, ○, ●, sintering TiO_2Sb containing, respectively, 0.1, 1.0, and 1.5% of Sb from Eq. (*16*).

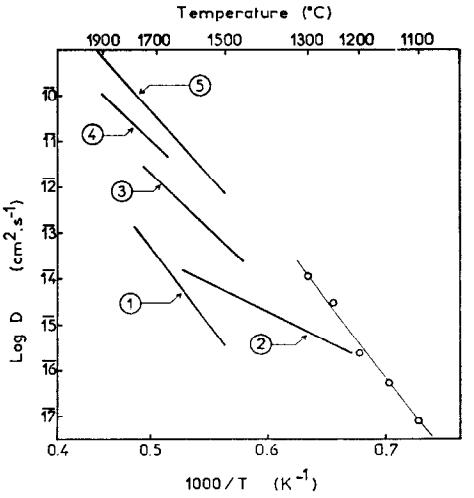

FIG. 5. Comparison of the diffusion coefficients calculated from the sintering data of Al_2O_3 with the diffusion data in the literature. Curves 1, 2 and 3: ^{18}O in Al_2O_3 (*27*). Curve 4: ^{26}Al in Al_2O_3 (*26*). Curve 5: sintering Al_2O_3 (*5*). O, sintering Al_2O_3 (this study) from Eq. (*16*).

$$D = 52.7 \exp\left(\frac{-77330}{RT}\right) \text{cm}^2 \text{sec}^{-1}$$

for temperatures between 700°C and 800°C.

(c) TiO_2B: Heterogeneous Particles

In the case of compacts made with heterogeneous particles the isothermal shrinkage as a function of time can be expressed by an equation of the form:

$$\frac{\Delta L}{L_0} = kt^n$$

with $n = 0.33$ between 620 and 700°C and $n = 0.38$ between 750 and 840°C. An intermediate value $n = 0.35$ is observed for 730°C.

Although the geometry of the system under study is very far from the geometry of the model, the values of D_v (volume diffusion coefficient) and $b\,D_B$ (grain boundary diffusion coefficients multiplied by the grain boundary width) have been calculated from Eq. (13) (Figs. 4 and 6, respectively):

$$D_v = 4.5 \exp\left(\frac{-72510}{RT}\right) \text{cm}^2 \text{sec}^{-1}$$

$$bD_B = 1.6 \times 10^{-8} \exp\left(\frac{-61720}{RT}\right) \text{cm}^3 \text{sec}^{-1}.$$

Moreover, as the value of n (0.38) is very close to the value given by Kingery and Berg (*6*), the apparent diffusion coefficient D has been calculated from Eq. (10) in order to compare the results with results obtained from Eqs. (13), (15), and (16) (Fig. 4):

$$D = 7.2 \times 10^{-2} \exp\left(\frac{-68300}{RT}\right) \text{cm}^2 \text{sec}^{-1}.$$

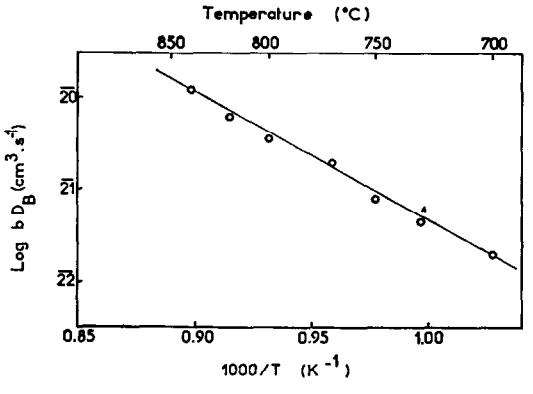

FIG. 6. Product of the grain boundary diffusion coefficient and grain boundary width calculated for TiO_2B from Eq. (*16*).

Discussion

The activation energy of sintering for all samples of titanium dioxide under study varies between 72 and 77 kcal/mole. These values are very close to the values obtained by Whitmore and Kawai (*20*) (74 kcal/mole) and Anderson (*21*) (77 kcal/mole) in the case of the sintering of rutile particles 0.35 μm in diameter and by O'Brian and Parravano (*22*) (68 kcal/mole) in the case of rutile spheres 1 mm in diameter. All of these values are of the same order of magnitude as those determined by the study of the isotopic exchange reaction for the diffusion of oxygen in rutile (*23*) (60 to 75 kcal/mole) and somewhat higher than the value for the diffusion coefficient of ^{44}Ti in rutile (61.6 kcal/mole (*24*), 59.9 kcal/mole for D_{zz}, and 48.5 kcal/mole for D_{xx} (*25*)).

A comparison of the diffusion coefficients calculated from the sintering experiments of titanium dioxide with the values given in the literature (Fig. 4) shows that values obtained with spherical particles of titanium dioxide and with antimony-doped titanium dioxide are about 10 times as high as the oxygen diffusion coefficient in rutile (*23*) determined in the same temperature range. However, these values are in good agreement with the values extrapolated from ^{44}Ti diffusion data (*24, 25*). The rate-controlling process of sintering should be the diffusion of the cation.

This conclusion is supported by a comparison of the diffusion coefficient calculated from the sintering data of δ-alumina with the diffusion data in the literature (Fig. 5) (*26*, 27). Indeed these values are higher than the value of the diffusion coefficient of oxygen in alumina, but are of the same order of magnitude as the extrapolated values of the diffusion coefficient of aluminum. They are also very close to the data obtained by Kuczynski (*5*) by measurement of the neck growth between spheres of alumina.

In the case of the sintering of heterogeneous particles of titanium dioxide (TiO_2 *B*), the apparent diffusion coefficient D_v calculated from the Eq. (13) compares favorably with the results obtained from spherical particles. On the other hand, diffusion coefficients calculated from Eq. (10) are in good agreement with the diffusion coefficient of oxygen, but neither this equation, nor Eq. (13) can be applied in this case: the first because of the inappropriate assumption in the derivation and both because the geometrical model does not fit the experimental system.

Conclusion

Kinetic equations of sintering, established from simple geometric models, must be used with caution in the case of heterogeneous samples of poorly defined particles. In some cases, an apparent agreement can be found between the theoretical and experimental laws, but it must be considered as fortuitous when all hypotheses underlying the theoretical laws are not satisfied. More refined mathematical treatments would not lead to improvements of the calculated values of the diffusion coefficient as long as the geometry of the system under study remains far from the theoretical geometry involved in the model.

By choosing a suitable model and by using well-defined particles of alumina and of pure or antimony-doped titania, it can be concluded that, in the case of these oxides, the mass transport, during sintering, is controlled by the cation diffusion.

References

1. M. Astier and P. Vergnon, *Rev. Int. Hautes Tempér. Réfract.* **9**, 265 (1972).
2. C. Herring, "The Physics of Powder Metallurgy," p. 153, McGraw-Hill, New York/Toronto/London, (1951).
3. G. C. Kuczynski, *Trans. A.I.M.E.* **185**, 169 (1949).
4. G. C. Kuczynski, *J. Appl. Phys.* **21**, 632 (1950).
5. G. C. Kuczynski, L. Abernethy, and J. Allan, "Kinetics of High Temperature processes," p. 147, MIT Press, Cambridge, Mass. (1959).
6. W. D. Kingery and M. Berg, *J. Appl. Phys.* **26**, 1205 (1955).
7. R. L. Eadie, D. S. Wilkinson, and G. C. Weatherley, *Acta Metallurg.* **22**, 1185 (1974).
8. R. L. Eadie and G. C. Weatherly, *Scripta Metallurg.* **9**, 285 (1975).
9. G. Cizeron, *C.R. Acad. Sci.* **244**, 2047 (1957).
10. J. Dequenne, *Rev. Int. Hautes Tempér. Réfract.* **10**, 141 (1973).
11. D. L. Johnson, *Phys. Sintering* **113**, 131 (1969).
12. D. L. Johnson, *J. Appl. Phys.* **40**, 192 (1969).
13. P. Vergnon, M. Astier, and S. J. Teichner, "Sintering and Related Phenomena," p. 301, Plenum Press, New York/London, (1973).
14. F. W. Vahldiek, D. E. Swihart, and S. A. Mersol, "Sintering and Related Phenomena," p. 617, Gordon and Breach, New York/London/Paris, (1967).
15. F. R. N. Nabarro, Report of a Conference on the strength of Solids, p. 75, Physical Soc. London, (1948).
16. C. Herring, *J. Appl. Phys.* **21**, 437 (1950).
17. M. Formenti, F. Juillet, P. Meriaudeau, S. J. Teichner, and P. Vergnon "Aerosol and Atmospheric Chemistry," p. 45, Academic Press, New York (1972).
18. P. Vergnon, M. Astier, D. Beruto, G. Brula, and S. J. Teichner, *Rev. Int. Hautes Tempér. Réfract.* **9**, 271 (1972).
19. P. Vergnon, M. Astier, and S. J. Teichner, "Fine Particles," p. 299, Electrochem. Soc. Inc., Princeton, (N.J.), (1974).
20. D. H. Whitmore and T. Kawai, *J. Amer. Ceram. Soc.* **45**, 375 (1962).
21. H. U. Anderson, *J. Amer. Ceram. Soc.* **50**, 235 (1967).
22. H. M. O'Bryan Jr. and G. Parravano, *Mater. Sci. Eng.* **1**, 177 (1966).
23. R. Haul, D. Just and G. Dümbgen, "Reactivity of Solids," Proc. 4th Intern. Symp. React. Solids, Amsterdam, 1960, p. 65, Elsevier, Amsterdam, (1961). R. Haul and G. Dümbgen, *Z. Elektrochem.* **66**, 636 (1962). R. Haul and G. Dümbgen, *J. Phys. Chem. Solids* **26**, 1 (1965).
24. D. A. Venkatu and L. E. Poteat, *Mater. Sci. Eng.* **5**, 258 (1969/1970).
25. T. S. Lundy and W. A. Coghlan, *J. Physique* **34**, Suppl., C9-299 (1973).
26. A. E. Paladino and W. D. Kingery, *J. Chem. Phys.* **37**, 957 (1962).
27. Y. Oishi and W. D. Kingery, *J. Chem. Phys.* **33**, 48 (1960).